

Nanoporous Linear Polyethylene from a Block Polymer Precursor

Louis M. Pitet, Mark A. Amendt, and Marc A. Hillmyer*

Department of Chemistry, University of Minnesota, Minneapolis, Minnesota 55455

Received February 3, 2010; E-mail: hillmyer@umn.edu

Porous polymer membranes are important for ultrafiltration and other size selective separation applications.¹ For example, lithium ion batteries incorporate porous polyolefins to prevent direct anode–cathode contact without compromising ionic conductivity.² Effective battery separators should be tough and chemically robust and have a combination of high porosity and small pore sizes.³ Development of next generation nanoporous polyolefins with optimized attributes is desirable considering the emphasis on high-energy-density lithium ion batteries for wide ranging applications. In this communication we demonstrate that nanostructured block polyolefins containing a sacrificial component are particularly attractive precursors to such advanced membranes.⁴ We describe the preparation of robust nanoporous membranes derived from perfectly linear polyethylene (LPE)–polylactide (PLA) triblock copolymers. Our membrane preparation protocol exploits disordered bicontinuous morphologies induced by the well-entangled, highly PLA-incompatible and crystallizable LPE. We show that chemically and mechanically robust LPE membranes with controlled pore sizes and high void fractions are accessible by this approach.

Nanoporous polyethylene has been generated from hydrogenated polybutadiene (hPB)–polystyrene block polymers from anionic polymerization by a harsh and difficult to control etching technique to remove polystyrene.⁵ Also, nanoporous hPB membranes have been derived from polymeric bicontinuous microemulsions.⁶ The unavoidable presence of branches in hPB leads to reduced melting temperatures, lower crystallinity, and greater susceptibility to chemical degradation relative to LPE, which exhibits outstanding mechanical properties and chemical robustness. By combining polymerization mechanisms⁷ we prepared LPE block polymers containing a sacrificial block and generated nanoporous LPE from these ordered materials by a selective etching protocol.

We recently reported the combination of Ru-catalyzed ring-opening metathesis polymerization (ROMP)⁸ with a chain transfer agent (CTA) and Sn-catalyzed ROP of D,L-lactide for the formation of PLA-poly(cyclooctadiene)-PLA triblock copolymers.⁹ An analogous approach starting with ROMP of cis-cyclooctene (COE), which includes catalytic hydrogenation of hydroxytelechelic poly-

(cyclooctene), allows preparation of PLA-LPE-PLA (LEL) triblocks with controlled molecular weights and compositions (Scheme 1).

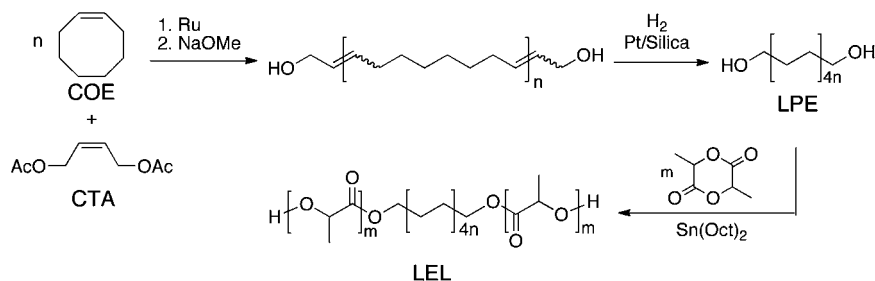
For this study, we evaluated LEL[37-28-37] and LEL[14-28-14], where the numbers designate the number average molar masses of the constituent blocks in kg/mol (Table S1 and Figures S1–S4). A sample of LEL[37-28-37] was compression molded at 160 °C. SAXS analysis (Figure S6) at 160 °C showed a broad signal with a maximum at 0.06 nm⁻¹ ($d = 105$ nm) with no discernible higher-order reflections consistent with a microphase separated structure lacking long-range order. We posit that the high degree of incompatibility between LPE and PLA¹⁰ combined with a low entanglement molecular weight for LPE¹¹ hinders the adoption of a well-organized mesophase. Annealing the samples up to 72 h at 160 °C did not appreciably increase the level of organization. Cooling from the melt to ambient temperature results in crystallization of the LPE phase (Figure S5). SAXS analysis for either sample at 25 °C (Figure S6) gave virtually indistinguishable profiles compared to the 160 °C data, which is indicative of confined LPE crystallization and consistent with behavior of other block polymers containing polyethylene (i.e., hPB) and a highly incompatible component.¹²

Exposure of molded LEL[37-28-37] samples to a 0.5 M solution of NaOH selectively removed the PLA, as confirmed gravimetrically and by IR spectroscopy (Figure S7). An interconnected LPE scaffold with a disorganized pore structure was observed by scanning electron microscopy (SEM) (Figures 1 and S8). Etched LEL[14-28-14] samples show a similarly disordered bicontinuous morphology (Figure S9) after PLA removal despite containing significantly less PLA compared to LEL[37-28-27].

Nitrogen adsorption analysis of nanoporous membranes derived from both samples showed type IV adsorption/desorption isotherms indicative of mesoporosity (Figure S10). Narrow pore-size distributions (BJH method; desorption isotherms) have maxima at 24 and 38 nm for nanoporous membranes from LEL[14-28-14] and LEL[37-28-37], respectively, with calculated peak widths at half-height equal to 3.5 and 11.1 nm (Figures 2 and S11). Specific surface areas calculated for LEL[14-28-14] and LEL[37-28-37] derived membranes were 70 and 96 m² g⁻¹, respectively.

Thin (~150 μm) films of the LEL samples were cast at 140 °C from tetralin for tensile testing evaluation (see Supporting Informa-

Scheme 1. Synthesis of LEL Triblock Polymer



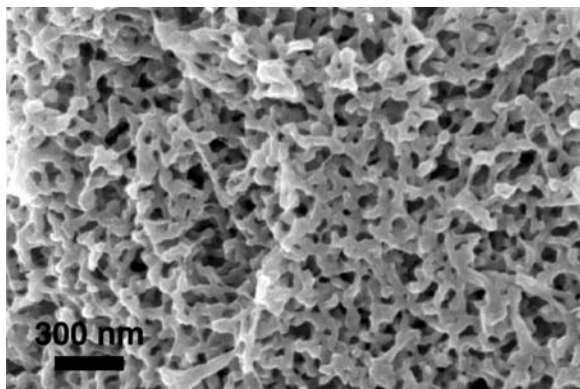


Figure 1. SEM image of a freeze-fractured surface from a sample of **LEL**[37-28-37] post-PLA removal (Pt coating \approx 2 nm).

tion). These solvent cast films adopt the same disordered bicontinuous morphologies as the molded samples as determined by SEM (Figure S12). From the stress–strain curves of these samples (Figure S13) we determined tensile toughness values of 1.54 and 4.91 MJ m⁻³ for nanoporous versions of **LEL**[37-28-37] and **LEL**[14-28-14], respectively; these values are comparable to those of tough nanoporous materials we recently prepared by a polymerization induced phase separation method (\sim 1.5 MJ m⁻³).¹³

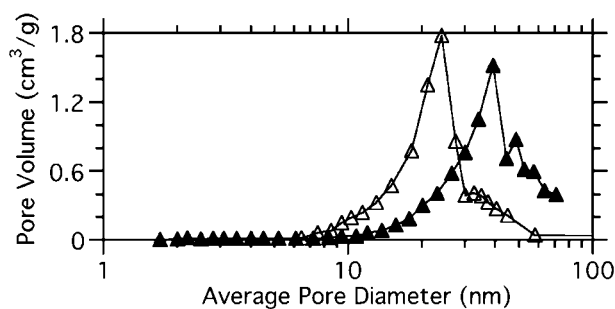


Figure 2. Pore-size distribution for porous LPE monoliths calculated from nitrogen desorption isotherms (differential pore volume). Empty triangles: **LEL**[14-28-14]. Filled triangles: **LEL**[37-28-37].

Temperature-induced pore collapse is an important attribute in battery separators for preventing thermal runaway and minimizing the potential for ignition upon fortuitous anode/cathode contact. The DSC analysis of the nanoporous LPE membranes (Figure S5 and Table S1) gave high melting temperatures ($T_{m,LPE} \approx 130$ °C) and levels of crystallinity ($X_{LPE} \approx 60\%$) as compared to typical values for hPB ($T_{m,hPB} \approx 105$ °C; $X_{hPB} \approx 40\%$).¹⁴ Annealing the nanoporous LPE membranes at 150 °C for 5 min causes pore collapse as confirmed by SEM analysis (Figure 3).

Finally, chemical resistance to strong acids was evaluated by submerging sections of the **LEL**[37-28-37] derived nanoporous samples into concentrated sulfuric (@ RT), hydrochloric (@ 50 °C), and nitric (@ RT) acids for 24 h. After rinsing and drying, >95% of the mass was retained in all cases. By SEM, there was little difference in the pore structure at the exposed surface (Figure S14) in both the sulfuric and nitric acid cases. After the HCl treatment the porosity and pore size distribution were

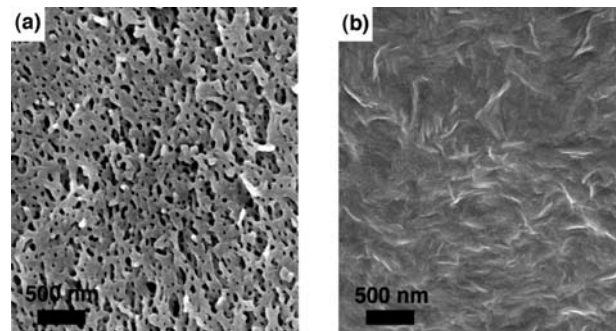


Figure 3. SEM images for membrane derived from **LEL**[14-28-14] (a) before and (b) after annealing at 150 °C for 5 min.

minimally affected according to nitrogen adsorption analysis (Figure S15).

The membranes prepared from the **LEL** block polymer templates reported in this communication hold tremendous promise for battery separator and other demanding separation applications. The bicontinuous morphologies adopted by the **LEL** samples allow for preparation of nanoporous membranes of various sizes/thicknesses with the level of porosity dictated by the block polymer composition. Most notably, the membranes exhibit the appealing chemical and thermal stability of exemplary LPE materials.

Acknowledgment. This work was supported by the National Science Foundation (DMR-0605880). Parts of this work were carried out at the University of Minnesota Characterization Facility, a member of the NSF-funded Materials Research Facilities Network (www.mrfn.org). SAXS was performed at Beamline 5 (DND-CAT) at Argonne National Laboratory. We thank Prof. Michael Tsapatsis for use of the nitrogen adsorption apparatus and are grateful to Dr. Liang Chen for invaluable discussions.

Supporting Information Available: Synthetic details and Figures S1–S15. This material is available free of charge via the Internet at <http://pubs.acs.org>.

References

- (1) Ulbricht, M. *Polymer* **2006**, *47*, 2217–2262.
- (2) Arora, P.; Zhang, Z. *Chem. Rev.* **2004**, *104*, 4419–4462.
- (3) Zhang, S. S. *J. Power Sources* **2007**, *164*, 351–364.
- (4) For relevant reviews: (a) Olson, D. A.; Chen, L.; Hillmyer, M. A. *Chem. Mater.* **2008**, *20*, 869–890. (b) Hillmyer, M. A. *Adv. Polym. Sci.* **2005**, *190*, 137–181.
- (5) (a) Uehara, H.; Yoshida, T.; Kakiage, M.; Yamanobe, T.; Komoto, T.; Nomura, K.; Nakajima, K.; Matsuda, M. *Macromolecules* **2006**, *39*, 3971–3974. (b) Uehara, H.; Kakiage, M.; Sekiya, M.; Sakuma, D.; Yamanobe, T.; Takano, N.; Barraud, A.; Meurville, E.; Ryser, P. *ACS Nano* **2009**, *3*, 924–932.
- (6) Jones, B. H.; Lodge, T. P. *J. Am. Chem. Soc.* **2009**, *131*, 1676–1677.
- (7) (a) Myers, S. B.; Register, R. A. *Macromolecules* **2008**, *41*, 5283–5288. (b) Switek, K. A.; Chang, K.; Bates, F. S.; Hillmyer, M. A. *J. Polym. Sci., Part A: Polym. Chem.* **2007**, *45*, 361–373.
- (8) Bielawski, C. W.; Grubbs, R. H. *Prog. Polym. Sci.* **2007**, *32*, 1–29.
- (9) Pitet, L. M.; Hillmyer, M. A. *Macromolecules* **2009**, *42*, 3674–3680.
- (10) Schmidt, S. C.; Hillmyer, M. A. *J. Polym. Chem., Part B: Polym. Phys.* **2002**, *40*, 2364–2376.
- (11) Fetters, L. J.; Lohse, D. J.; Richter, D.; Witten, T. A.; Zirkel, A. *Macromolecules* **1994**, *27*, 4639–4647. (a) Loo, Y.-L.; Register, R. A.; Ryan, A. J. *Macromolecules* **2002**, *35*, 2365–2374.
- (12) (b) Castillo, R. V.; Müller, A. J.; Lin, M.-C.; Chen, H.-L.; Jeng, U. S.; Hillmyer, M. A. *Macromolecules* **2008**, *41*, 6154–6164.
- (13) Chen, L.; Phillip, W. A.; Cussler, E. L.; Hillmyer, M. A. *J. Am. Chem. Soc.* **2007**, *129*, 13786–13787.
- (14) Ryan, A. J.; Hamley, I. W.; Bras, W.; Bates, F. S. *Macromolecules* **1995**, *28*, 3860–3868.

JA100985D